

CHARACTERISTICS AND PHENOL RED ADSORPTION CAPACITY IN AQUEOUS SOLUTIONS OF SBA-15 ADSORBENT SYNTHESIZED FROM THE ASH OF BRICKYARD

Tran Hoai Lam^{1*}, Nguyen Van Hoa¹, Tran Thi Thanh Truc²,
Truong Tien Dung³, Le Minh Hoa³, Nguyen Phan Duyen Nu²,
Giang Ngoc Ha¹, Nguyen Hoc Thang¹

¹*Ho Chi Minh City University of Food Industry*

²*SGS Vietnam Ltd., Ho Chi Minh City*

³*Kengta Technologies Ltd., Ho Chi Minh City*

*Email: lamth@hufi.edu.vn

Received: 16 December 2021; Accepted: 15 April 2022

ABSTRACT

The ash of brickyards or rice husk ash is a big problem for the environment, and it is necessary to have good solutions to manage and utilize as a raw material for other industries. In addition, the organic wastes with high solubility in water have been also causing many bad consequences to human health, animals, and plants. Therefore, this study used the ash of brickyard to synthesize SBA-15 materials known as adsorbents in removal of organic wastes like as phenol red out of aqueous solutions. The experimental results showed that the SBA-15-based nanomaterials had well-ordered hexagonal meso-structure and its pore diameter was approximately 7.8 nm. The nano-adsorbents of SBA-15 had also high adsorption of the phenol red. The experimental data on phenol red adsorption were evaluated based on the Langmuir isotherm model and the pseudo-second-order model well with high regression coefficients at $R^2 = 0.9995$ and 0.9900 , respectively. The phenol red adsorption efficiency of SBA-15-based nanomaterials was really high at 98.8 % and its maximum adsorption capacity reached to 19.77 mg.g⁻¹.

Keywords: SBA-15, ash, phenol red, adsorption, and adsorbent.

1. INTRODUCTION

The Mekong Delta is the largest local on rice production in Vietnam with a total output around 40 million tons per year, accounting for 90% rice of the country [1]. In addition to the main product of rice, the rice harvest and processing have also generated a number of other by-products such as rice husk and straw in very large quantities. This poses a challenge for the local people to manage and re-use these by-products. In fact, there have been many solutions such as using them to compost or burn to get fertilizer with low efficiency. The rice husk has been used as a solid fuel in several agricultural drying kilns with high construction and installation costs. More specifically in the Mekong delta, there are also many factories producing burnt-clay bricks using fuelwood or coal for combustion. However, the prices of these fuels are really high and continuously increasing. Therefore, these local facilities have been used rice husk and straw to replace for traditional fuels during the burning process. The burning processes has produced a lot of solid wastes, which are the non-combustible inorganic components in rice husk or straw known as the ash of brickyard. Many production facilities

have dumped the solid wastes on their farmland without any solution to reuse it. There have been many studies shown that the ash of brickyard contains high silica of SiO₂. Normally, after burning, the ash has over 80% is silicon oxide with amorphous reactive silica [2]. Thus, this is a potential resource, which has many different applications in fields of materials science. The silica from rice husk ash has been used in rubber [3], adsorbents [4], filter materials [5], etc. This study utilized the ash of brickyard as a raw material to synthesize nano-adsorbents which aim to improve the environmental pollution and wastewater treatment. It is noted that there is no study on nano-adsorbents based on silica from the ash of brickyard.

Phenol red or phenolsulfonphthalein exists as a red crystal with the aqueous solubility at 0.77 g.L⁻¹. The phenol red solution was often used as a pH indicator in cell culture [6] and as a dye. The eyes, respiratory system, and skin may be irritated after exposed to phenol red [7]. In addition, the phenol red is also able to cause inhibition of the growth of renal epithelial cells [7]. It is toxic to muscle fibres and have mutagenic effects [8, 9]. Therefore, the impacts of phenol red on the environment should be investigated and must have a good solution for its treatment. There have been many investigations on using various materials to adsorb phenol red such as the bottom ash and deoiled soya adsorbents [10]; and clinoptilolite [11]. In addition, many reports also used the various models to evaluate adsorption capacity and adsorption efficiency in wastewater treatment with the synthesized materials such as silica material [12], modified bentonite [13], and others [14, 15].

The SBA-15 adsorbents have been researched with outstanding specifications such as high surface area around 900 m².g⁻¹; high thermal and mechanical stability; inert and environmentally friendly properties [16]. The SBA-15 materials are normally synthesized from tetraethoxysilane (TEOS) as the silica source with high cost and complex TEOS processes [17- 18]. This is motivation to enhance the development of alternative silica sources known as the rice husk ash or the ash of brickyard. Thus, this study focused on two main investigations included utilization of the brickyard ash as a raw material for synthesizing SBA-15 nano-adsorbent and its experiments on the phenol red adsorption in aqueous solutions. It is noted that the microstructural characteristics of SBA-15 nanomaterials were analysed using Fourier transform infrared spectroscopy (FTIR), X-ray diffraction (XRD), transmission electron microscopy (TEM), Brunauer–Emmett–Teller (BET). The absorption capacity and absorption of SBA-15 nano-adsorbents were recorded during the removal of phenol red dye.

2. MATERIALS AND METHODS

2.1. The ash of brickyard

The raw material was from the local burnt-clay brick production facilities in Mekong delta, Vietnam. The brickyard ash was prepared via the processes of drying, sieving to remove the soil, sand, rock, and other contaminants, and grinding as reported in Nguyen (2019) [2].

2.2. Chemical reagents

This study used the chemical reagents of NaOH, HCl, Phenol red and Pluronic P123 (Amphiphilic triblock copolymer poly(ethylene oxide)-poly-(propylene oxide)-poly(ethylene oxide, MW=5800) from Merck Vietnam Ltd.

2.3. Preparation of SBA-15 mesoporous materials

Figure 1 is a diagram of the experimental steps from the preparation of raw materials for the synthesis of SBA-15 nanomaterials to the analyses of the microstructural characteristics and the phenol red absorption efficiency in aqueous solution of the product.

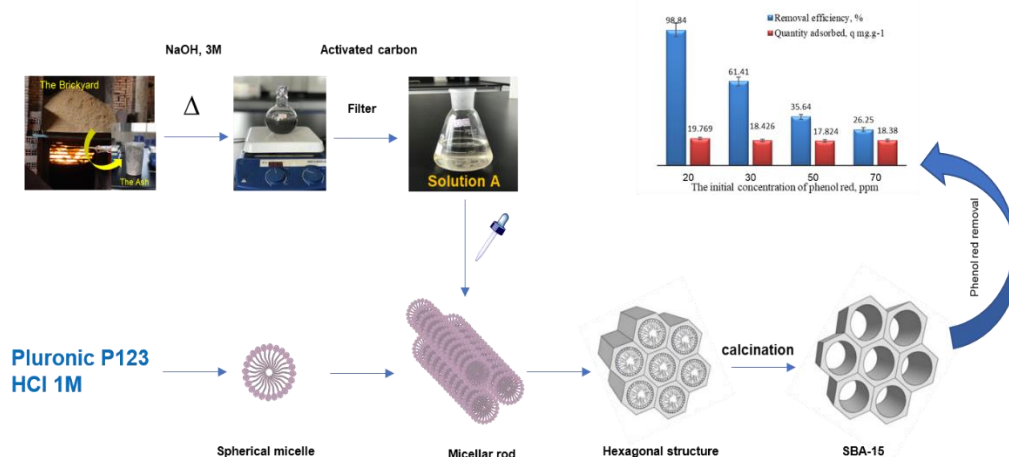


Figure 1. Preparation of SBA-15 nano-adsorbent with microstructural characteristics and its phenol red absorption efficiency.

For each experiment, the ash with 10 g was soaked in 150ml of 3M NaOH solution and stirred at temperature of 110 °C for 3 hours. Then, the sample was filtered using activated carbon to obtain a colourless solution (solution A). In other work, the Pluronic P123 surfactant was dissolved in an aqueous solution of 1M HCl at room temperature (solution B). The next step, solution A was added on a drop-by-drop into solution B to form a precipitate. The whole mixture was put into a glass jar and incubated at temperature of 105 °C for 24 hours to obtain gel. And then, the white precipitate was filtered and washed with water to neutral and dried at 105 °C for 24 hours. The sample was removed surfactant by calcining at 550 °C with heating rate at 10 °C/min in the atmosphere condition [19].

Finally, the nanomaterial of SBA-15 was characterized for microstructure and morphologies using methods of FTIR, XRD, TEM, BET with nitrogen adsorption-desorption.

Both samples of P-SBA-15 without calcination and SBA-15 with calcination were analysed to detect the functional groups of chemical bondings using FTIR (8400S Shimadzu with KBr pellets).

The SBA-15 sample was characterized for the phase compositions using method of X ray diffraction (XRD) with the diffraction angle of 2-Theta from 0.5 to 80° and a step size of 0.02. The experiments were conducted at German-Vietnamese Technology Academy, Ho Chi Minh City University of Food Industry (GVTA-HUFI) using Bruker D2 diffractometer and Research & Experiment Center, Vietnam Petroleum Institute (REC-VPI) using Bruker D8 Advance diffractometer with CuK_α radiation ($\lambda=1.54 \text{ \AA}$).

The specific surface area and total pore volume of the SBA-15 nano-adsorbent sample were analysed by nitrogen adsorption-desorption isotherms at 77 °K using Quantachrome Nova 2000e meter.

2.4. Preparations for phenol red adsorption

A beaker was prepared with 200 mL aqueous solution of phenol red. And then, 2 g nano-adsorbent of SBA-15 was added in the beaker. The different adsorbent concentrations were adjusted at 20 ppm, 30 ppm, 50 ppm, and 70 ppm. The sample was stirred for 180 minutes and then the concentrations of phenol solution were determined using UV-Vis spectrophotometry.

2.5. Interpretation of adsorption isotherm model

The Langmuir isotherm model was used to analysed the sorption equilibrium data for the phenol red on SBA-15 nano-adsorbent [20, 21]. The relative coefficients of the model were calculated using linear least-squares fitting.

The Langmuir sorption isotherm equation is known as follows:

$$q_e = Q_m K_L C_e / (1 + k_L C_e) \quad (1)$$

and it is linearized to become:

$$\frac{C_e}{q_e} = \frac{C_e}{Q_m} + \frac{1}{Q_m k_L} \quad (2)$$

where, q_e (mg g⁻¹) and C_e (mg L⁻¹) are the equilibrium concentrations of phenol red in the nano-adsorbent of SBA-15 and liquid phases, respectively; Q_m and k_L are the Langmuir constants which are related to sorption capacity and energy of sorption, respectively, and they are calculated from the intercept and slope of the linear plot of C_e/q_e and C_e .

2.6. Kinetic models

The pseudo-second-order were used to analyse the sorption kinetic data for cobalt on the various adsorbents [22]. The pseudo-second-order equation was written into:

$$\frac{dq_t}{dt} = k_2 (q_e - q_t)^2 \quad (3)$$

where, k_2 (g.mg⁻¹.min⁻¹) is the rate constant; q_t and q_e (mg g⁻¹) are the amount of sorption at time t (min) and at equilibrium, respectively.

The equation (3) is integrated and applied for the above conditions to become:

$$\frac{1}{q_e - q_t} = \frac{1}{q_e} + k_2 t \quad (4)$$

After rearranged, the equation (4) changes into a linear form:

$$\frac{t}{q_t} = \frac{1}{k_2 q_e^2} + \frac{1}{q_e} t \quad (5)$$

in which, k_2 and q_e are obtained from the intercept and slope of the plot t/q_t and t , respectively.

3. RESULTS AND DISCUSSION

3.1. Characteristics of the adsorbent based on SBA-15 synthesized from the ash of brickyard

The FTIR spectra of samples are shown in Figure 2. The bands observed at wavenumbers of 1080 cm⁻¹, 804 cm⁻¹ and 484 cm⁻¹ corresponding to bend stretching vibrations of Si–O–Si with symmetric and asymmetric, respectively. At the wavenumber of 960 cm⁻¹, it was resulted from Si–OH stretching band. The broad band of wavenumbers from 3000 to 3700 cm⁻¹ is vibrations of hydroxyl groups. The sharp peak at 3745 cm⁻¹ is related to the vibrations of the Si–OH. Figure 2a for the P-SBA-15 sample without calcination had the wavenumber at 2800 cm⁻¹ detected to vibrations of C-H bonding. It is noted that Figure 2b for the SBA-15 sample with calcination had no peak at wavenumber of 2800 cm⁻¹. The results showed that the framed organic fraction with Fluronic P123 was successfully removed by calcination at temperature of 550 °C for 5 hours.

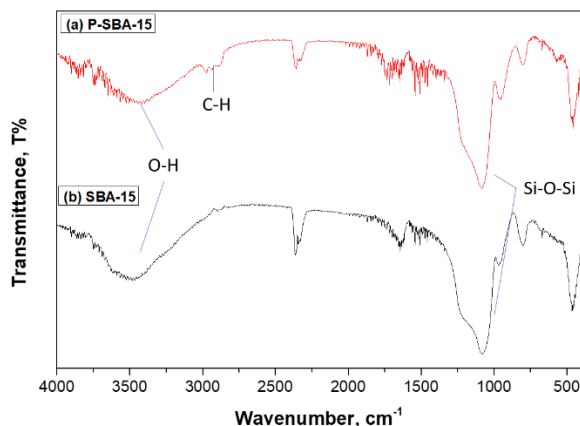


Figure 2. Vibrations of the chemical functional groups in P-SBA-15 (a) and SBA-15 (b) using FTIR.

The XRD patterns of SBA-15 nano-adsorbent are shown in Figure 3. In Figure 3a, the peaks of SBA-15 sample were detected at 2-Theta of 1.0° , 1.7° , and 1.9° characterized for crystal planes (100), (110), and (200), respectively. The results are suitable to the previous studies on SBA-15 based materials using TEOS as raw material in the synthesized processes [16-18]. The peak with narrow and high intensity of crystal planes (100) of in SBA-15 sample indicated a good mesopore ordering and the typical hexagonal channels of SBA-15 based materials [17]. In Figure 3b, the wide angle XRD pattern of SBA-15 indicates that the nanomaterial has high silica with major amorphous structure due to noisy and broad background of the XRD pattern. There is a peak at 2-Theta of 22.5° which is diffraction of silica crystals. This is a characteristic hexagonal structure of SBA-15 based materials as shown in Figure 1.

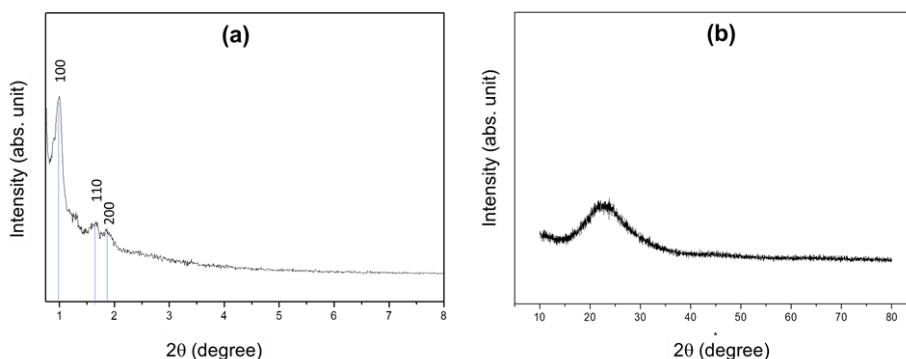


Figure 3. XRD patterns of SBA-15 based nano-adsorbent at small-angle X-ray scattering (a) and wide-angle region X-ray scattering (b).

The morphologies and microstructural characteristics of adsorbent based on SBA-15 was observed by transmission electron microscopy (TEM) using a JEM JEOL – 1400 microscope instrument (Japan) with an acceleration voltage of 100 kV. The TEM images showed that the particles of SBA-15 have the sizes about 8 nm with the really uniform distribution as shown in Figure 4. In addition, the TEM nano-graphs showed that the sample of SBA-15 had a long order and uniform channel structures along to pores axes and hexagonal cross sections. This is a really convincing scientific evident on the nanostructures of SBA-15 synthesized from the brickyard ash. These results are consistent with that of the XRD patterns in Figure 3 and the previous investigations on SBA-15 synthesized from TEOS raw material [16-18].

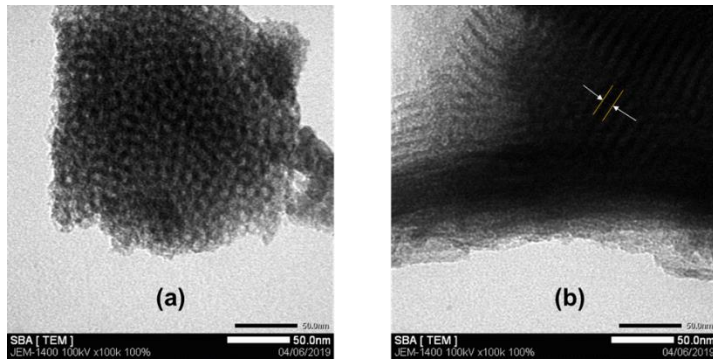


Figure 4. Nanostructures of SBA-15 sample using TEM with normal to pore axis (a) and along to pore axis (b).

The pore size distribution of SBA-15 is shown in Figure 5 with the analysis of desorption branch of the isotherm by the BJH method. In which, the pore sizes have high distribution in range of 50 Å to 100 Å equivalent to 5-10 nm. The surface area was determined at 772.224 m².g⁻¹, pore volume of 0.838 cm³.g⁻¹, and pore diameter at 7.8 nm. These results are similar to nanostructures detected by TEM in Figure 4.

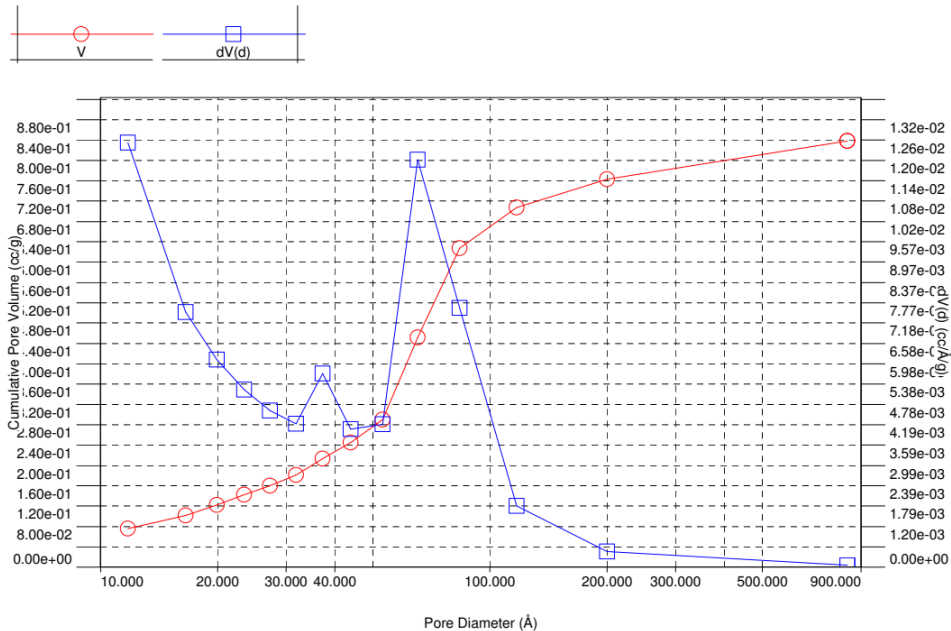


Figure 5. The pore size distribution of the SBA-15 nanomaterial using BET with BJH method.

3.2. The phenol red adsorption in aqueous solutions of SBA-15 nanomaterial

3.2.1. The effect of time

In general, the adsorption capacity and adsorption efficiency of the adsorbent based SBA-15 significantly rose with increasing stirring time. As shown in Figure 6, the phenol red adsorption of SBA-15 adsorbent rapidly increased in the first 20 minutes, and then it slightly rose until 150 minutes. Finally, the phenol red adsorption capacity of the SBA-15 insignificantly slowly increased and the equilibrium was achieved at 180 minutes when the adsorption sites were filled out.

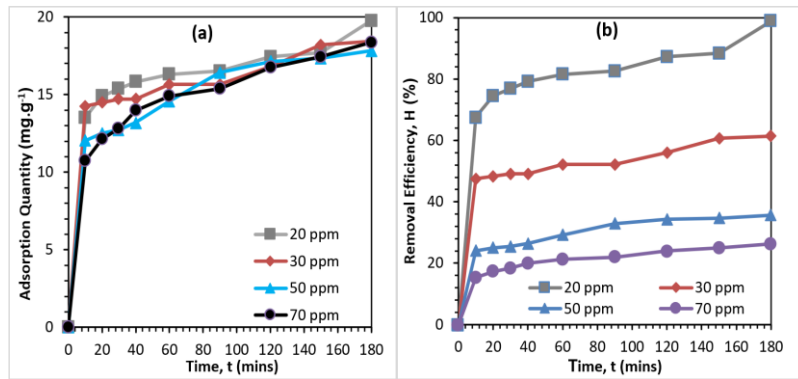


Figure 6. Effects of time on the phenol red adsorption of SBA-15 adsorbent with the adsorption quantity (a) and removal efficiency (b).

The experimental data showed that the longer stirring time had, the more phenol red adsorption increased. However, this is only suitable for stirring time less than 180 minutes. The phenol red adsorption capacity and adsorption efficiency are not influenced or less effected by the stirring time when it is over 180 minutes. The highest adsorption capacity reached at was 19.77 mg.g⁻¹ for the adsorption time of 180 minutes corresponding to the adsorption efficiency over 98.84 % as shown Figures 6b and 7.

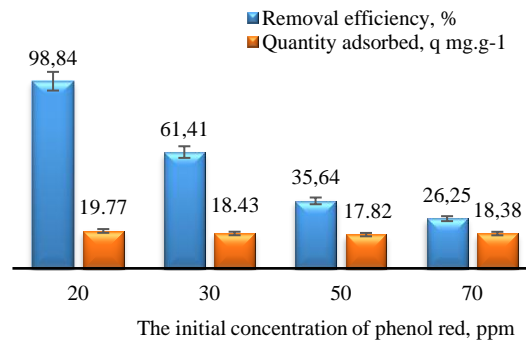


Figure 7. Effects of the phenol red concentrations on the adsorption capacity and removal efficiency of SBA-15 adsorbent.

3.2.2. Effect of initial phenol red concentration to removal efficiency

The phenol red adsorption of SBA-15 adsorbent was carried out in the different concentrations of 20 ppm, 30 ppm, 50 ppm, and 70 ppm with the stirring time at 180 minutes as shown in Figure 7. The phenol red adsorption has the highest values at 19.77 mg.g⁻¹ corresponding to the removal efficiency of 98.84% with the concentration of 20 ppm. When increasing the concentration of phenol red, the phenol red removal efficiency of SBA-15 adsorbent decreased sharply. Moreover, in this case, the adsorbed phenol red quantity changed insignificantly. The results indicated that the phenol red adsorption process on SBA-15 nano-adsorbent is the physical adsorption.

3.2.3. Langmuir isotherm model for phenol red adsorption

The phenol red sorption isotherm of SBA-15 adsorbent at room temperature is shown in Figure 8a. The sorption data were determined in term of Langmuir isotherm model. The results and graphical isotherm showed the fit with the Langmuir model with R² at 0.9995. The fitted constants for the Langmuir model are q_{max} at 18.315 mg.g⁻¹ and K_L at 8.4 L.mg⁻¹ as well as the regression coefficient of R² at 0.9995.

In Table 1 below, we summarize the results of previously published studies relevant to this topic. These results shown that, the phenol red adsorption capacity of SBA-15 materials is higher other materials.

Table 1. The phenol red adsorption capacities of various adsorbents

No.	Adsorbents	The phenol red adsorption capacity, q_{max} [mg.g ⁻¹]	References
1	SBA-15	18.315	This study
2	Activated carbon	6.756	[11]
3	Bottom ash	9.214	[10]

3.2.4. The kinetic for the phenol red adsorption of SBA-15 adsorbent

The experimental adsorption kinetic data were fitted to pseudo-second-order rates as mentioned in Equation (5). The linear observation of lines in Figure 8b indicated that the adsorption kinetic data are well represented by the pseudo-second-order model for phenol red with the regression coefficient of R^2 over 0.994. This was applied for all concentrations conducted experiments in this study.

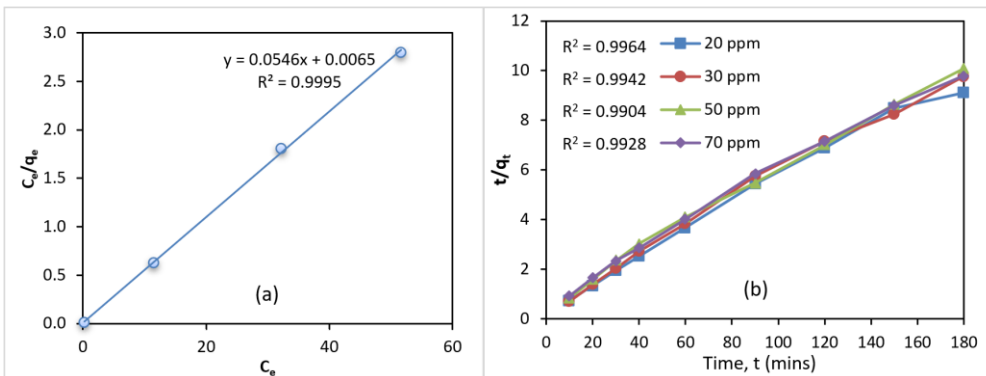


Figure 8. The phenol red adsorption of SBA-15 adsorbent responding to Langmuir sorption isotherm model (a) and pseudo-second-order sorption kinetic model (b).

4. CONCLUSIONS

The adsorbent of SBA-15 was successfully synthesized from the ash of brickyard with the microstructural characteristics responding to nanomaterial requirements. The results of nitrogen adsorption/desorption and TEM nano-graphs illustrated the formation of cylindrical pores and a well-ordered hexagonal array of SBA-15 adsorbent. In which, the nanomaterial has the high specific surface area of 772.224 m².g⁻¹, pore volume of 0.838 cm³.g⁻¹ and average pore size at 7.8 nm. The SBA-15 adsorbent has high ability to remove the phenol red in aqueous solutions with the removal efficiency up to 98.84%. And the maximum adsorbed phenol red quantity of SBA-15 nanomaterial is at 19.77 mg.g⁻¹. The phenol red adsorption process of SBA-15 adsorbent was the physical adsorption. The experimental data of phenol red adsorption were satisfied well to the Langmuir isotherm model with high regression coefficient of R^2 at 0.9995. Moreover, the pseudo-second-order model also met to apply the exchange kinetic data of the phenol red adsorption process with regression coefficient of R^2 over 0.99. Future research will be carried out for improvements of SBA-15 adsorbent to achieve the better output parameters in wastewater treatment. In addition, the adsorbent of

SBA-15 based on the brickyard ash should be also conducted experiments related to the adsorption of heavy metals in aqueous solutions to clean the polluted environment.

Data Availability: The data used to support the findings of this study are available from the corresponding author upon request.

Conflicts of Interest: The authors declare that there is no conflict of interest regarding the publication of this paper.

Funding Statement: This work was financially supported by Ho Chi Minh City University of Food Industry (Project No. ĐTKHCNGV.017/2020).

Acknowledgments: The authors would like to thank to Labs of Faculty of Chemical Technology (HUFIT) supported for doing experiments in this research.

REFERENCES

1. <https://www.gso.gov.vn/default.aspx?tabid=621&ItemID=19454>
2. Hoc Thang Nguyen - synthesis and characteristics of inorganic polymer materials geopolymerized from ash of brickyard, *Materials Science Forum* **961** (2019) 45-50. <https://doi.org/10.4028/www.scientific.net/MSF.961.45>.
3. Chang B.P, Gupta A., Muthurai R., Mekonnen T. - Bioresourced fillers for rubber composite sustainability: current development and future opportunities, *Green Chemistry* **23** (2021) 5337–5378., 2021. <https://doi.org/10.1039/D1GC01115D>
4. Donanta Dhaneswara, Jaka Fajar Fatriansyah, Frans Wensten Situmorang, Alfina Nurul Haqoh - Synthesis of amorphous silica from rice husk ash: Comparing HCl and CH₃COOH acidification methods and various alkaline concentrations, *International Journal of Technology* **11** (2020) 200-208. <https://doi.org/10.14716/ijtech.v11i1.3335>
5. Madu J. O., Adams F. V., Agboola B. O., Ikotun B. D., Joseph I. V. - Purifications of petroleum products contaminated water using modified rice husk ash filters, *Materials Today: Proceedings* **38** (2021) 599-604. <https://doi.org/10.1016/j.matpr.2020.03.466>
6. Yolande Berthois, John A. Katzenellenbogen, and Benita S. Katzenellenboge - Phenol red in tissue culture media is a weak estrogen, *Proceedings of the National Academy of Sciences of the United States of America* **83** (1986) 2496-2500. <https://doi.org/10.1073%2Fpnas.83.8.2496>
7. Walsh-Reitz M. M., Toback F. G. - Phenol red inhibits growth of renal epithelial cells, *American Journal of Physiology* **262** (1992) 687-691. <https://doi.org/10.1152/ajprenal.1992.262.4.f687>
8. Chung K. T., Fulk G. E., Andrews A. W. - Mutagenicity testing of some commonly used dyes, *Applied and Environmental Microbiology* **42** (1981) 641–648. <https://doi.org/10.1128/aem.42.4.641-648.1981>
9. Baylor S. M., Hollingworth S. - Changes in phenol red absorbance in response to electrical stimulation of frog skeletal muscle fibers, *Journal of General Physiology* **96** (1990) 449–471. <https://doi.org/10.1085%2Fjgp.96.3.473>
10. Mittal A., Kaur D., Malviya A., Mittal J., Gupta V. K. - Adsorption studies on the removal of coloring agent phenol red from wastewater using waste materials as adsorbents, *Journal of Colloid and Interface Science* **337** (2009) 345–354. <https://doi.org/10.1016/j.jcis.2009.05.016>

11. Alebachew N., Yadav O. P., Lokesh - Removal of phenol red dye from contaminated water using barley (*Hordeum vulgare* L.) husk-derived activated carbon, *Science International* **5** (2017) 7–16. <http://dx.doi.org/10.17311/sciintl.2017.7.16>
12. Tran Hoai Lam, Nguyen Van Du, Quach Nguyen Khanh Nguyen, Nguyen Minh Thao – Adsorption of Pb^{2+} và Cu^{2+} ions in aqueous solution by silica materials synthesized from the ash of brickyard, *Journal of Analytical Sciences* **24** (2019) 8-15. (in Vietnamese)
13. Nguyen L. M. L., Tran D., Hoang V. D., et al. - Phenol Red Adsorption from Aqueous Solution on the Modified Bentonite, *Journal of Chemistry* **2020** (2020) ID 1504805. <https://doi.org/10.1155/2020/1504805>
14. Amar A., Loulidi I., Kali A., Boukhlifi F., Hadey C., Jabri M., - Physicochemical Characterization of Regional Clay: Application to Phenol Adsorption, *Applied and Environmental Soil Science* **2021** (2021) ID 8826063. <https://doi.org/10.1155/2021/8826063>
15. Hoc Thang Nguyen, Dang Thanh Phong - Using Activated Diatomite as Adsorbent for Treatment of Arsenic Contaminated Water, *Key Engineering Materials* **850** (2020) 16–23. <https://doi.org/10.4028/www.scientific.net/KEM.850.16>
16. Hoang V.T., Huang Q., Eic M., Do T. O., Kaliaguine S. - Structure and diffusion characterization of SBA-15 Materials, *Langmuir* **21** (2005) 2051-2057. <https://doi.org/10.1021/la048349d>
17. Ryoo R., Ko C. H., Kruk M., Antochshuk V., Jaroniec M. - Block-copolymer-templated ordered mesoporous silica: Array of uniform mesopores or mesopore–micropore network?, *The Journal of Physical Chemistry B* **104** (2000) 11465–11471. <https://doi.org/10.1021/jp002597a>
18. Zhao D., Sun J., Li Q., Stucky G.D. - Morphological control of highly ordered mesoporous silica SBA-15, *Chemistry Materials* **12** (2000) 275-279. <https://doi.org/10.1021/cm9911363>
19. Quach Nguyen Khanh Nguyen, Nguyen Thi Yen, Nguyen Duc Hau, and Hoai Lam Tran - Synthesis and characterization of mesoporous silica SBA-15 and ZnO/SBA-15 photocatalytic materials from the ash of brickyards, *Journal of Chemistry* **2020** (2020). <https://doi.org/10.1155/2020/8456194>
20. Yu C., Fan J., Tian B., Zhao D. - Morphology development of mesoporous materials: a colloidal phase separation mechanism, *Chemistry Materials* **16** (2004) 889-898. <https://doi.org/10.1021/cm035011g>
21. Glasstone S. - Text book of physical chemistry, 2nd edition, Macmillan, India, 1981.
22. Ho Y.S., Mckay G. - Pseudo-second order model for sorption processes, *Process Biochemistry* **34** (1999) 451-465. [https://doi.org/10.1016/S0032-9592\(98\)00112-5](https://doi.org/10.1016/S0032-9592(98)00112-5)

TÓM TẮT

ĐẶC TÍNH VÀ KHẢ NĂNG HẤP PHỤ PHENOL ĐỎ CỦA VẬT LIỆU SBA-15 ĐƯỢC TỔNG HỢP TỪ TRO LÒ GẠCH

Trần Hoài Lam^{1*}, Nguyễn Văn Hòa¹, Trần Thị Thanh Trúc²,
Trương Tiến Dũng³, Lê Minh Hòa³, Nguyễn Phan Duyên Nữ²,
Giang Ngọc Hà¹, Nguyễn Học Thắng¹

¹ Trường Đại học Công nghiệp Thực phẩm TP.HCM

² Phòng Kiểm tra chất lượng, Công ty SGS Việt Nam

³ Công ty Kỹ thuật Kengta Việt Nam

*Email: lamth@hufi.edu.vn

Tro thải lò gạch hay tro trấu là một vấn đề lớn của môi trường, do đó cần phải có một giải pháp tối ưu để quản lý và sử dụng nó làm nguyên liệu cho nhiều ngành sản xuất khác. Hơn nữa, các chất thải hữu cơ tan trong nước nói chung và phenol đỏ nói riêng đã và đang gây ra nhiều hệ quả xấu đối với sức khỏe con người, động vật và cây cối. Trong nghiên cứu này, tro lò gạch đã được sử dụng để tổng hợp vật liệu SBA-15 và sử dụng làm chất hấp phụ để loại bỏ phenol đỏ ra khỏi dung dịch nước. Kết quả thực nghiệm cho thấy, vật liệu SBA-15 đã tổng hợp thành công với đường kính lỗ khoảng 7,8 nm. Quá trình hấp phụ phenol đỏ của chất hấp phụ SBA-15 tuân theo phương trình đẳng nhiệt hấp phụ Langmuir và phương trình động học hấp phụ bậc 2 với R^2 tương ứng 0,9995 và 0,9900. Dung lượng và hiệu suất hấp phụ tối đa của phenol đỏ là 19,77 mg.g⁻¹ và 98,84%.

Từ khóa: SBA-15, tro, phenol đỏ, sự hấp phụ, chất hấp phụ.